PHYSICAL REVIEW D VOLUME 43, NUMBER 4 15 FEBRUARY 1991

Global texture as the origin of large-scale structure: Numerical simulations of evolution

David N. Spergel
Princeton University Observatory, Peyton Hall, Princeton University, Princeton, New Jersey 08544

Neil Turok
Joseph Henry Laboratory, Princeton University, Princeton, New Jersey 08544

William H. Press and Barbara S. Ryden
Harvard-Smithsonian Center for Astrophysics, 60 Garden St., Cambridge, Massachusetts 02138
(Received 1 June 1990)

Numerical simulations explore the evolution of global texture in an expanding universe. The evolution is surprisingly simple—"knots," regions with a nonzero winding number, collapse and unwind at a fixed rate per horizon volume per horizon time; the comoving density of knots n unwinding in a conformal time interval $d\eta$ obeys $dn/d\eta \simeq 0.04\eta^{-4}$. During each collapse, asymmetries are damped and the texture knots appear to approach an exact spherically symmetric scaling solution. The locations of the knots are anticorrelated on scales smaller than the horizon scale and uncorrelated on larger scales. We calculate the density and pressure in the texture "scaling solution" in the matter and radiation eras. We estimate (in a universe dominated by cold dark matter with $\Omega=1$) that of order ten knots of angular radius of order 8° should be visible on the microwave sky.

I. INTRODUCTION

An intriguing pattern of very-large-scale structure in the Universe is emerging more and more clearly from observation. The currently popular theories of its origin "reveal a distinct lack of correlation" with the new results[1] and are close to being ruled out by observations of the microwave background.[2] In particular, the "standard" inflation plus cold-dark-matter model appears to be in conflict with a number of different observations of large-scale structure and could be ruled out in the future by microwave observations from the South Pole.[2]

In this paper we begin a systematic exploration of a new mechanism for producing large-scale inhomogeneities in an initially homogeneous universe—defects produced when non-Abelian global symmetries are broken. Here we shall consider the most generic such defect, global texture, discussed as a mechanism for the formation of galaxies and large-scale structure formation by Turok.[3] In subsequent papers we shall consider global monopoles[4] and "nontopological texture."[3]

Global texture is an unstable topological defect that arises whenever a non-Abelian globe symmetry is completely broken. Grand unified theories in which this occurs are simple to construct, and "family unification" schemes necessarily involve broken non-Abelian global symmetries.[3,5] The dynamics of the nonlinearly coupled Goldstone-boson fields constituting the texture is to an excellent approximation independent of any parameters, involving only the speed of light and the geometry of the vacuum manifold. This makes the theory highly predictive. The evolution of texture is completely independent of parameters and so, therefore, is the pattern into which the matter is perturbed by the gravitational attraction of the texture. To obtain the correct magnitude of density fluctuations today, one requires that the global symmetry be broken around the grand unified scale, a "natural" scale. With this breaking scale the Goldstone bosons which the texture is made out of are very weakly coupled to matter and would not be observed in laboratory experiments. Global texture does, however, produce a characteristic pattern on the microwave sky which may be observable in the near future.[5]

While historically there has been some prejudice in particle theory against broken global symmetries and the associated Goldstone bosons, they occur ubiquitously in condensed-matter systems, and the possibility of their occurrence at a more fundamental level is certainly worth exploring. Of course, it is also true that dynamics similar to that we describe here occurs in condensed-matter systems with similar symmetry-breaking patterns, for example, in liquid crystals.

Our main finding in this paper is that the evolution of global texture is remarkably simple. While the dynamics is highly nonlinear, it is largely governed by the topology of the field and it is quite accurately described by a low-resolution code. This makes possible the study of the full three-dimensional evolution over a large range of physical scales. We have extended a "leapfrog" computer code developed by Press, Ryden, and Spergel to study domain walls in an expanding universe[6] in order to study texture dynamics. The simplicity of the code (the central evolution algorithm occupies five lines) means that our results should be easy to reproduce—and the study of the cosmological effects of global defects should be almost as simple as that of the random Gaussian noise, a standard paradigm for initial fluctuations.

The plan of the paper is as follows. In Sec. II we re-

view the evolution of the simplest "SU(2)" global texture. In Sec. III we review the numerical techniques used to evolve the texture fields in an expanding universe and describe several tests of the code. Our results on the cosmological evolution of the simplest texture are described in Sec. IV. Section V sums up.

II. EVOLUTION OF TEXTURE

In three dimensions the simplest symmetry-breaking scheme which produces textures involves a global SU(2) symmetry broken by a Higgs doublet ϕ with the potential

$$V(\phi)=\lambda(2|\phi|^2-\phi_0^2)^2 , \quad (1)$$

just as in the Weinberg-Salam electroweak theory. Of course, in the latter case the SU(2) symmetry is gauged, whereas we shall consider the case where it is a global (ungauged) symmetry. A classic example of such a theory is Skyrme's model of pion dynamics.[7] The texture "knots" in that model were identified with nucleons and stabilized by the addition of higher-derivative terms to the action. Here we shall assume that such terms, if present, have little effect (we return to this point below).

By writing the complex doublet ϕ as a real four-vector $\phi=(1/\sqrt{2})(\phi_1+i\phi_2,\ \phi_3+i\phi_4)$, $\boldsymbol{\phi}\equiv(\phi_1,\ldots,\phi_4)$, one sees that V_0, the space of minima of $V(\phi)$, is a three-sphere $\boldsymbol{\phi}^2=\phi_0^2$. Of course, this is no accident, but rather the result of a general theorem that if a group G breaks to a subgroup H, then, barring accidental degeneracy, $V_0\approx G/H$. Here $G=\mathrm{SU}(2)$ and $H=1$, and so $V_0\approx\mathrm{SU}(2)\approx S_3$. In the broken-symmetry phase, there are three massless Goldstone-boson modes tangential to the three-sphere, and one massive radial "Higgs" mode, with a mass $m_\phi=\sqrt{8\lambda}\phi_0$. The inverse Higgs-boson mass m_ϕ^{-1} sets a length scale, which we shall frequently refer to as W_0.

A heuristic picture of texture evolution is as follows. We assume that the Universe starts out in a hot and homogeneous big bang (perhaps, but not necessarily, following a period of inflation). At high temperatures $T\gg\phi_0$, the symmetry is restored, and the long-wavelength modes of $\boldsymbol{\phi}$ are localized about $\boldsymbol{\phi}=0$. As the Universe cools, there is a phase transition and the global symmetry is broken. The Higgs field falls to the vacuum manifold, but winds around it in a nontrivial way on scales larger than the correlation length, which by causality must be smaller than the horizon. As Turok[3] argued, in such "winding" regions the field configuration collapses at the speed of light and, when the field gradients become large enough to lift ϕ over the potential barrier, "unwinds" itself in regions of radius W_0. As the Universe expands, the Higgs field becomes correlated on larger and larger scales. In this process gradient energy in the fields is converted into incoherent "Goldstone-boson" oscillatory modes, which then redshift away. Long after the phase transition (which occurs at around the grand unified scale), the scale on which coherent gradients occur in the Higgs field continues to grow at the speed of light, with the Hubble radius. We shall refer to this fixed point in the evolution of the texture field as the scaling solution. In the case of texture, the coherent field gradients are themselves a source of inhomogeneity, but there is the more dramatic effect of knot collapse as well. As the Universe expands, comoving regions in which the Higgs field winds around the vacuum manifold come across the horizon. These "knot" configurations collapse at the speed of light down to the scale W_0 where they unwind.[3] An analytic solution describing spherical collapse was found in Ref. 5. This collapse produces a roughly spherical overdense region onto which matter is attracted in a characteristic pattern.[5,8,9] Collapsing knots are, as we shall see, produced at a fixed rate per horizon time per horizon volume at all times right up to the present day. One of our more surprising findings is that they become remarkably spherical as the collapse proceeds, appearing to approach the analytic solution. The density fluctuations induced in dark matter by the collapse of a knot appear to fit quite well the $\delta\rho\propto r^{-1}$ profile predicted from spherical collapse in flat space.[5] We shall discuss this behavior in more detail in a forthcoming paper.[10]

This picture of the evolution of the texture field should apply quite generally to theories with broken global non-Abelian symmetries. What is required is that longest-wavelength "dynamical" modes, i.e., those of horizon wavelength, dominate the dynamics. This will be the case for theories producing global monopoles, for example, where the energy of the defects diverges linearly with scale and is thus dominated by the largest scales. It should also apply to "nontopological texture."[3] In both these cases we expect to see a scaling solution with a correlation length of order of the horizon scale. For global strings the energy per unit length diverges logarithmically, at small and large scales, and so there is important dynamics on scales much smaller than the horizon. One would expect global strings to behave much like gauged cosmic strings, where the correlation length on the long strings is of order of one-tenth of the horizon scale. The feature of a horizon scale correlation length common to global defects from non-Abelian groups makes them far more promising as a means of generating large-scale structure than cosmic strings, either gauged or global. The horizon scale at matter-radiation equality corresponds to a comoving scale of approximately $16\Omega^{-1}h^{-2}$ Mpc, which is certainly comparable to the scale of structure seen in redshift surveys for reasonable values of h and Ω.

These considerations apply to the classical dynamics of $\boldsymbol{\phi}$; it is conceivable that on scales of order W_0 higher-derivative terms in the effective action for the quantum theory are large enough to stabilize the "knots" and prevent them from unwinding. As mentioned before, this is what Skyrme assumed in order to stabilize nucleons. Even if this should occur here (one would have to go beyond perturbation theory to show it), the time scale for quantum-mechanical tunneling through the barrier would generically be of order of the grand unified time scale and negligible on the time scales we are interested in. Needless to say, stable "knots" would be a cosmological disaster, rapidly coming to dominate the Universe.

In an expanding universe with a cosmological expan-

sion factor $a(t)$, the equations of motion for the ϕ field take the form

$$\frac{\partial^2\boldsymbol{\phi}}{\partial\eta^2}+2\left[\frac{da}{d\eta}\right]\frac{1}{a}\frac{\partial\boldsymbol{\phi}}{\partial\eta}-\nabla^2\boldsymbol{\phi}=-a^2\frac{\partial V}{\partial\boldsymbol{\phi}}\ , \tag{2}$$

where conformal time η is defined by the relation $d\eta\equiv dt/a(t)$, and the spatial gradients are taken with respect to comoving coordinates. The equations of motion are thus a wave equation with a Hubble damping term on the left-hand side and a force term on the right-hand side, driving the field into minima of the potential.

On scales much larger than W_0, there are two equivalent descriptions of the dynamics. Since gradients are small compared to m_ϕ, the massive Higgs mode is only negligibly excited. The main players are the Goldstone modes, whose evolution may be described in two different ways. Either we can stick to the description in terms of a four-component field with potential (1), or we can just describe the three massless modes interacting in the "nonlinear σ model approximation".[11] In this approximation, $\boldsymbol{\phi}^2=\phi_0^2$ is treated as a constraint, and the dynamical equations become

$$\nabla^\mu\partial_\mu\boldsymbol{\phi}=-\frac{\partial_\mu\boldsymbol{\phi}\cdot\partial^\mu\boldsymbol{\phi}}{\phi_0^2}\boldsymbol{\phi}\ , \tag{3}$$

independent of the shape of $V(\phi)$ or the magnitude of ϕ_0. The main use of the σ model description is to demonstrate that the evolution of cosmic texture on large scales is insensitive to the symmetry-breaking scale or the form of the Higgs potential. This is what makes the theory predictive. While the *magnitude* of the density perturbations depends on ϕ_0, the *pattern* in which they are laid down is fixed by the evolution of the fields, which depends solely on the geometry of V_0 (fixed by the symmetry groups involved) and the background geometry of the spacetime.

The nonlinear σ model description breaks down when $\boldsymbol{\phi}$ changes winding number—the σ model becomes singular at these points. Here one must revert to the "potential" description—as mentioned, at the center of "winding" regions the field gradients become large enough to lift $\boldsymbol{\phi}$ from V_0 and change its winding number. This process takes a time of order W_0. While it is important that the σ model description exists, and for the vast majority of the time it is an excellent approximation to the true dynamics, in practice we have found it simpler to evolve $\boldsymbol{\phi}$ using the potential $V(\phi)$ with W_0 chosen to be a few grid spacings. This allows the entire evolution to proceed without singularities, and provided the scales of interest are much larger than the grid spacing, the evolution should well approximate the nonlinear σ model anyway. We shall check this in Sec. III. In addition, the "potential" description allows us to set up initial conditions which mimic the thermal phase transition rather well and, in particular, enforce the "isocurvature" nature of the perturbations on scales larger than the initial horizon. The initial conditions we used were to set $\boldsymbol{\phi}=0$, but $d\boldsymbol{\phi}/d\eta$ a vector of random direction but fixed magnitude at each grid point. This choice of initial conditions means that the initial density is exactly uniform. It correctly enforces the isocurvature nature of the perturbations and avoid introducing random noise on scales larger than the horizon size in a noncausal way, as has been a problem for cosmic-string calculations (for a recent discussion, see Ref. 12). Of course, we expect that the long-term evolution of the field is insensitive to the details of the initial conditions, as long as they assign $\boldsymbol{\phi}$ randomly to points on V_0 on scales larger than the causal horizon.

It may be helpful to describe the "winding" of $\boldsymbol{\phi}$ around the three-sphere more precisely. As long as $\boldsymbol{\phi}$ remains on the three-sphere, there is a conserved topological current[7]

$$j^\mu=\frac{1}{12\pi^2\phi_0^4}\epsilon^{\mu\nu\alpha\beta}\epsilon^{abcd}\phi^a\partial_\nu\phi^b\partial_\alpha\phi^c\partial_\beta\phi^d\ . \tag{4}$$

The spatial integral $Q=\int d^3x\, j^0$ is constant as long as $\boldsymbol{\phi}$ remains on the three-sphere and if $\boldsymbol{\phi}$ is constant on the boundary of the integration region. It is an integer if $\boldsymbol{\phi}$ is parallel everywhere on the boundary. j^0 is therefore a "winding density." We shall somewhat loosely use the term "knot" to describe a causally connected region within which $Q=\int d^3x\, j^0\approx 1$ and "antiknot" for a region within which $Q=\int d^3x\, j^0\approx -1$. A rough criterion for collapse is that $Q>\frac{1}{2}$ or $Q<-\frac{1}{2}$, at least in the spherical and initially static case. It is hard to define knots more precisely. We shall often define them *post hoc* as regions where the Higgs field wrapped around in such a way as to lead to an unwinding event. We find collapses by looking for places where $\boldsymbol{\phi}^2$ falls significantly below ϕ_0^2. In the cases we examined, this corresponded to regions where $\boldsymbol{\phi}$ had wrapped most of the way around the three-sphere.

III. NUMERICAL TECHNIQUES

The fields were evolved according to Eq. (2) with the same code used to study domain walls in the expanding Universe,[6] now modified to treat multicomponent fields. Our evolution of a field with textures in an expanding universe encountered the same numerical difficulty discussed in the work with domain walls. The spatial grid is of constant comoving size, while the width of a topological defect such as a wall is constant in physical units and thus decreases in comoving units at the rate $a(t)^{-1}$. The topological defects have to be a few grid lengths thick in order to be resolved and cannot be permitted to shrink away to nothing. In order to bypass this problem, as in Ref. 6, we modified the equations of motion to

$$\frac{\partial^2\boldsymbol{\phi}}{\partial\eta^2}+\alpha\left[\frac{da}{d\eta}\right]\frac{1}{a}\frac{\partial\boldsymbol{\phi}}{\partial\eta}-\nabla^2\boldsymbol{\phi}=\frac{\partial V}{\partial\boldsymbol{\phi}}\ , \tag{5}$$

ignoring the a^2 factor on the right-hand side of (2). As was argued in Ref. 6, if one sets $\alpha=3$ instead of 2, Hubble damping of the massive modes has the same scaling in a matter-dominated universe in both Eqs. (2) and (5). If the dynamics are dominated by these modes, this is a reasonable procedure. Visual comparisons of domain-wall simulations based on Eqs. (3) and (5) revealed that

the macroscopic evolution of the walls was unaffected by the alteration of the equation. Short-wavelength oscillations along the walls, which were evident in the constant physical size simulations, were somewhat suppressed in the constant comoving size simulations. Kawano,[13] using a very different numerical technique that simulated the evolution of infinitely thin walls, also found evidence for short-wavelength wall oscillations. Otherwise, his results confirmed the results in Ref. 6 based on Eq. (5).

However, in the case of texture, the massless modes dominate, and it is better to use the original value $\alpha=2$. We argue below that since the massless modes dominate, it is nevertheless reasonable to ignore the a^2 term which should be present on the right-hand side of (5). We have therefore used $\alpha=2$ throughout. We evolve Eq. (5), with V as in (1), by a standard finite-difference scheme, staggered leapfrog for the second order in time term and Crank-Nicholson for the first-order term [for full details of the numerical method, see Ref. 6, Eqs. (32)–(35)].

In the case of texture, this procedure of scaling the potential with a^{-2} is more easily justified. This is because during the vast majority of its evolution, ϕ remains very close to V_0. The important modes are the Goldstone modes, which are unaffected by the shape or height of $V(\phi)$, and depend solely on the geometry of V_0, as explained above. Scaling the potential has the result that the "unwinding" regions remain constant in comoving size as the simulation proceeds. This scale rapidly becomes smaller than that on which most of the evolution is occurring, the horizon scale which (in comoving units) grows as a in the radiation era or $a^{1/2}$ in the matter era. As a check of this argument, we performed simulations with different values of W_0. The main effect of increasing W_0 was to lengthen the initial "roll-down" time; otherwise, the results were nearly identical. Changing the value of α did, however, significantly alter the results. We also compared our three-dimensional code with a high-resolution one-dimensional leapfrog code for the nonlinear σ model spherical collapse.

The computer simulations of the ϕ field were performed on a Cartesian grid with periodic boundary conditions. We performed three-dimensional simulations with 60^3 and 100^3 grids. We also ran two-dimensional simulations for a three-component field with vacuum manifold $V_0=S_2$, with slab boundary conditions (i.e., a three-dimensional periodic boundary condition simulation with a box height of one grid spacing) on a 800^2 grid. In all the simulations, the initial value of the field was fixed at $\phi=0$ and the initial velocity chosen to point in a random direction with fixed magnitude $|d\phi/d\eta|=\phi_0/\eta$. The correct isotropic measure on the two- or three-sphere was used. We evolved the fields with a constant conformal time step of 0.2 grid units in all the simulations and with an initial comoving horizon scale η of one grid unit (we use units where the speed of light is unity throughout).

To test the accuracy of the three-dimensional code and to see how well it followed the nonlinear σ model in ex-

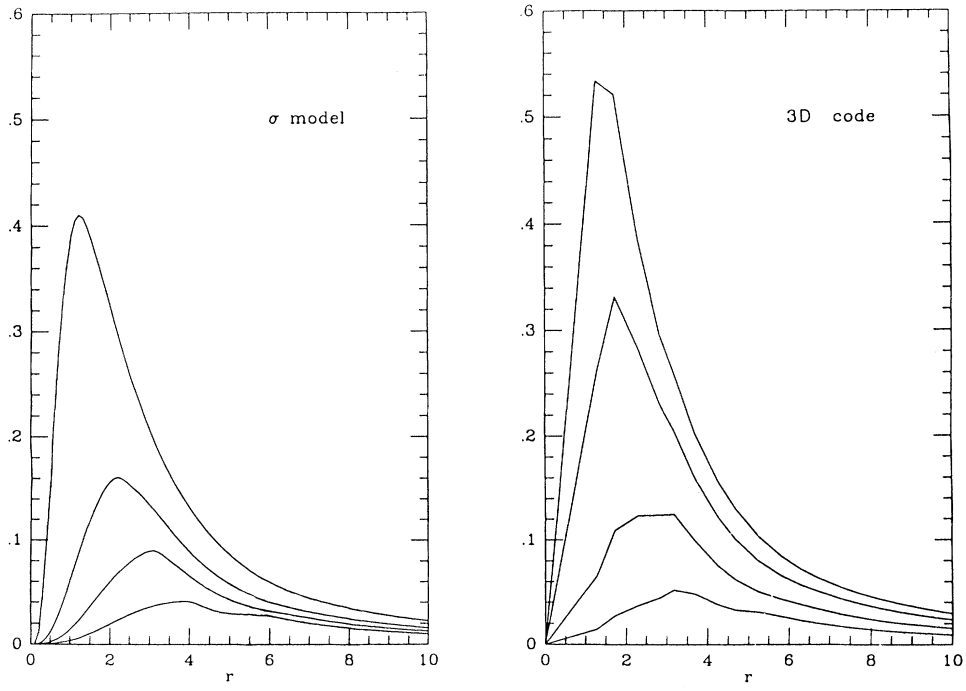

FIG. 1. Test of the three-dimensional code against a high-resolution spherical code for the nonlinear σ model. We calculate the effective acceleration of a test particle at comoving radius r from the center of collapse. This is plotted at one, two, three, and four units of conformal time η after the initial time $\eta=1$. On the left is the σ model code, on the right the three-dimensional code. The initial knot size was five units, and the three-dimensional code had $W_0=2$.

panding background, we wrote a standard leapfrog code to evolve the nonlinear σ model spherical solution in expanding backgrounds. This code reproduced the exact flat-spacetime solution found by two of us[5] to very high precision and was, in fact, how we discovered it. The spherical ansatz used was

$$\phi=(\cos\chi,\ \sin\chi\cos\theta,\ \sin\chi\sin\theta\cos\phi,\ \sin\chi\sin\theta\sin\phi)\ ,$$

with θ and ϕ the standard polar angles and $\chi(r,\eta)$ the single radial function. For a single isolated knot, χ varies from 0 at the origin to π at infinity. The σ model equations are, in this case,

$$\frac{\partial^2\chi}{\partial\eta^2}+2\left[\frac{da}{d\eta}\right]\frac{1}{a}\frac{\partial\chi}{\partial\eta}-\frac{\partial^2\chi}{\partial r^2}=-\frac{\sin(2\chi)}{r^2}\ . \tag{6}$$

The initial conditions used for the field were $\partial\phi/\partial\eta=0$ and χ increasing linearly with r with slope such that it reached π at a radius corresponding to five grid spacings in the three-dimensional code (with W_0 equal to two grid spacings). The results of the comparison are shown in Fig. 1, for a matter era background. We plotted the quantity most relevant to structure formation calculations: the effective acceleration produced on a test particle at comoving radius r at each time. This is given, in synchronous gauge, by GM/r^2, where M is the effective gravitating mass within radius r:

$$M=4\pi\int_0^r r^2dr(\rho+3p)=4\pi\int r^2dr\,2\dot{\phi}^2\ .$$

As usual, we ignored the potential contribution in the three-dimensional code. The spherical code used 100 spatial grid points, and the result it gave was very close to that with 400 grid points. As can be seen, the three-dimensional code performs acceptably well for textures only slightly larger than our resolution scale W_0. While the precise details are different, both the time of collapse and the shape of the acceleration field are very similar. With larger textures the agreement was even better.

As direct tests of the three-dimensional code, we evolved the same initial conditions in 60^3 boxes with W_0 of two and four grid spacings, respectively. The results are described in Sec. IV.

IV. NUMERICAL RESULTS

The numerical simulations tested the scaling behavior of texture evolution and determined the relevant numerical coefficients. As we explained above, as the Universe expands, the texture field corelates itself on a scale which grows with the horizon. In this scaling solution, the density in texture should remain a fixed fraction of the background density, $\rho\propto t^{-2}$, and the number of knots collapsing and unwinding per horizon volume per horizon time should remain constant.

In the simulations we computed the mean pressure and density in the ϕ field (averaged over the simulation volume):

$$P=a^{-2}[\tfrac{1}{2}\dot{\phi}^2-\tfrac{1}{6}(\nabla\phi)^2]\ , \tag{7}$$

and

$$\rho=a^{-2}[\tfrac{1}{2}\dot{\phi}^2+\tfrac{1}{2}(\nabla\phi)^2]\ , \tag{8}$$

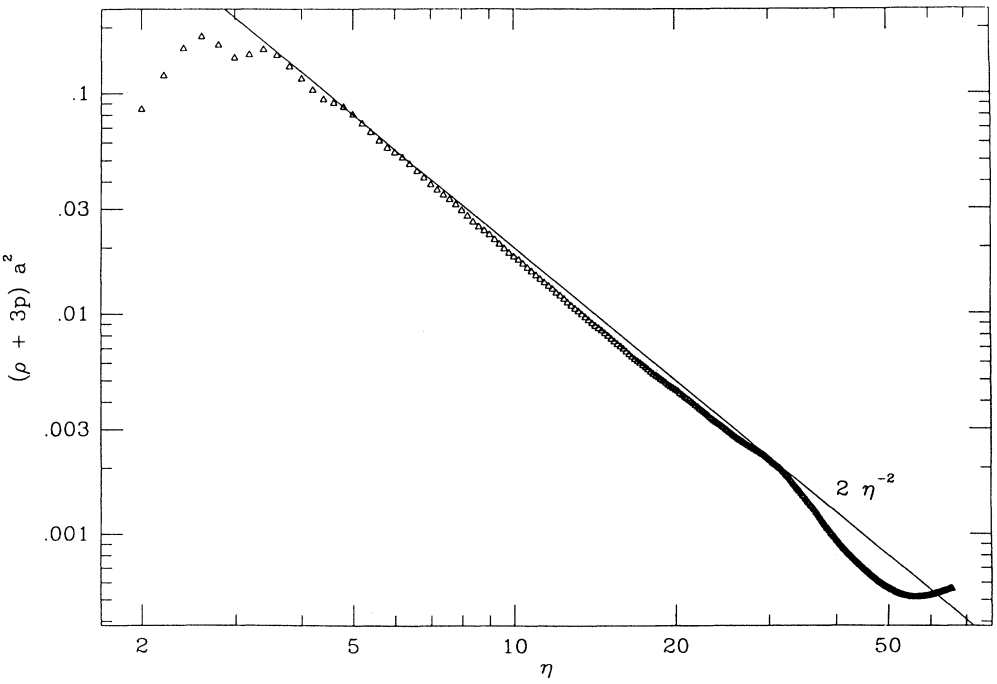

FIG. 2. Scaling with conformal time of the spatial average of the effective source density for perturbations in nonrelativistic matter in the matter era for a 100^3 simulation. The dashed line shows $2(\partial_\eta\phi)^2=2\phi_0^2/\eta^2$ (we use units where $\phi_0=1$).

where derivatives are with respect to conformal time and comoving coordinates. Since the potential plays little role outside of unwinding regions of radius W_0, we ignore its contribution to P and ρ (we justify this below in Fig. 3). Of particular interest is the scaling of the quantity $\rho+3P=2a^{-2}\dot{\phi}^2$, which, as we mentioned before, is the source for scalar mode density perturbations in synchronous gauge. Figure 2 shows this quantity plotted against conformal time $\eta \propto t^{1/3}$ in the matter era, calculated in a 100^3 matter era run. It obeys the predicted scaling very well. In Fig. 3 we show that P/ρ is small, and so the $3P$ term actually contributes very little. This is as required by stress-energy conservation—if the texture density scales as matter, the mean pressure should be zero. Furthermore, the numerical value $\dot{\phi}^2 \approx (\partial_x \phi)^2 \approx (\partial_y \phi)^2 \approx (\partial_z \phi)^2 \approx \phi_0^2/\eta^2$ indicates that the correlation length really is the horizon scale. As a direct check of energy conservation and its dependence on the parameter W_0, we calculated the value of P/ρ as well (in 60^3 runs). Figure 3 shows the evolution of P/ρ in the matter era for different values of W_0. As can be seen from the figure, doubling W_0 has little effect on the evolution after an initial transient. As we mentioned, "scaling" behavior requires $P=0$. In fact, we found P/ρ to be less than 0.05, an acceptable error. We also show that the average potential energy density $V(\phi)$ is a very small fraction of the total density in this figure.

Our results are consistent with the scaling solution

$$\rho \simeq 2\frac{\phi_0^2}{a^2\eta^2} \quad \text{(matter era)} . \tag{9a}$$

We also ran simulations in the radiation era. The results for $\rho+3P$ are shown in Fig. 4, where a comparison between a 100^3 and a 60^3 simulation is shown. In the scaling solution a fixed fraction of the total density in the Universe should be dumped into Goldstone modes each expansion time. Because these modes redshift at the same rate as the background, the fractional density in Goldstone radiation should grow logarithmically with time. Figure 5 shows the same quantity as in Fig. 3, but with a logarithmic correction $\ln(\eta/W_0)$ supposed to represent the logarithmic growth beginning after the initial transient "roll-down" phase, which lasts for a conformal time of order W_0. After this correction the agreement with the scaling prediction for both values of W_0 is excellent. Our results again confirm the scaling solution

$$\rho \simeq 2\frac{\phi_0^2 \ln(\eta/W_0)}{a^2\eta^2} \quad \text{(radiation era)} . \tag{9b}$$

We have not quoted errors on these results, because to do so might be misleading. Statistical errors are certainly small, but it is likely that the largest source of error is systematic and due to numerical inaccuracy. An estimate of these errors would require more detailed comparisons of the code run at different resolutions, whereas we have so far only performed the few simple tests shown above. Based on these tests, we believe that our results for the density and pressure in texture are unlikely to be wrong by more than 50%.

Our results conform with the scaling behavior expected, indicating that the power spectrum in the density fluctuations should be approximately of the Harrison-Zel'dovich form, i.e., constant amplitude at horizon crossing.

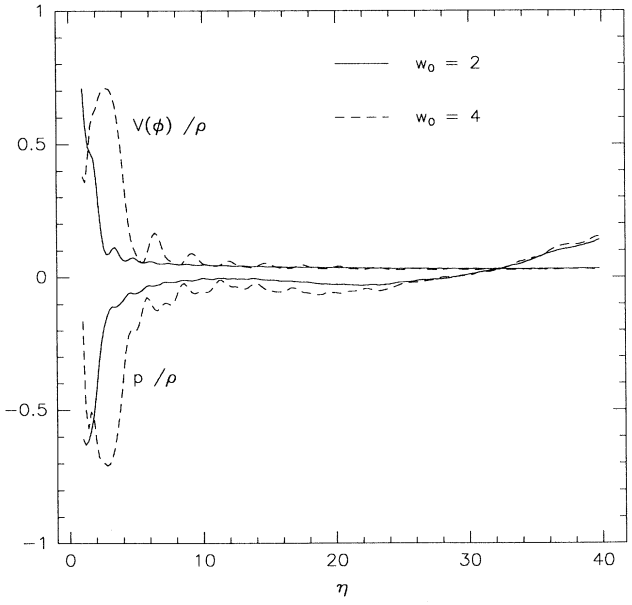

FIG. 3. Average value of P/ρ as a function of conformal time for two 60^3 runs in the matter era with different values of W_0. Also shown is the value of the average potential energy density $V(\phi)/\rho$, confirming the argument in the text that after a short time this becomes negligible.

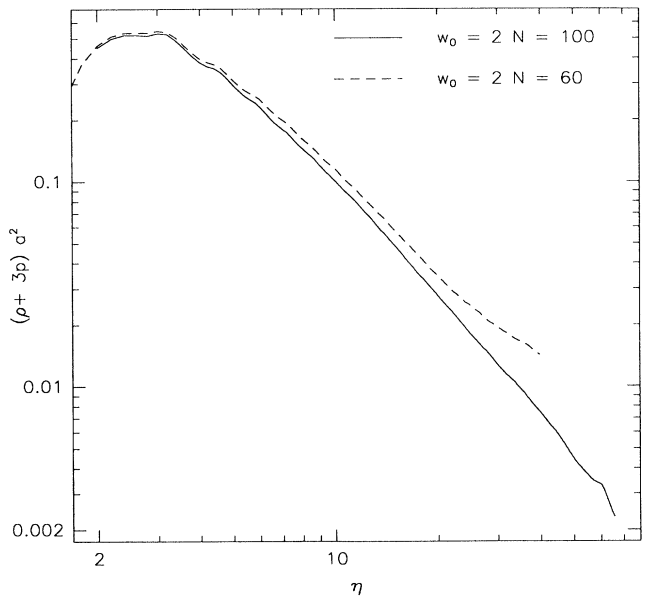

FIG. 4. Scaling with conformal time of the spatial average of the effective source density for perturbations in nonrelativistic matter in the radiation era for a 100^3 and a 60^3 simulation.

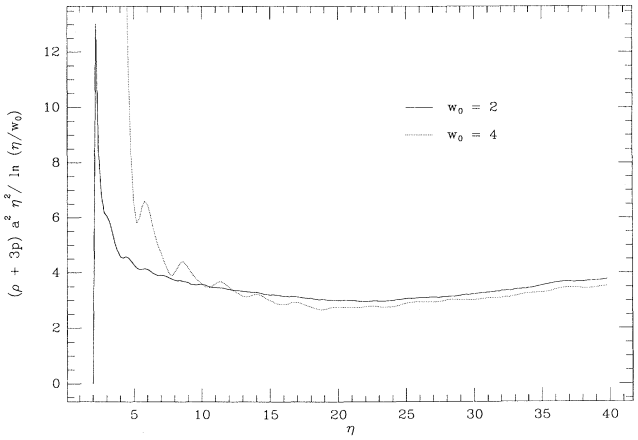

FIG. 5. Same quantity as in Fig. 3, but for 60^3 runs in the radiation era and including the logarithmic correction explained in the text. Again, the results for $W_0=2$ and 4 are virtually indistinguishable at late times.

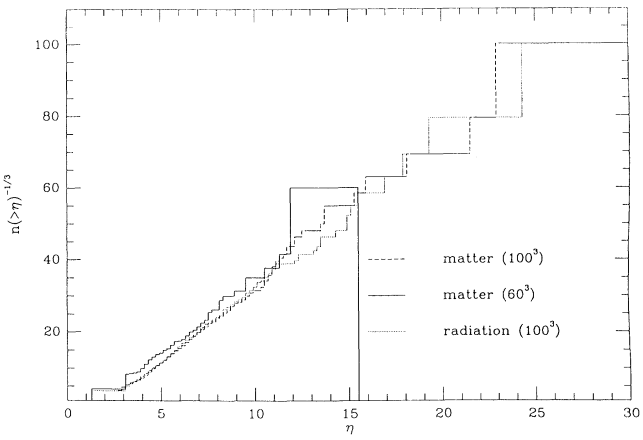

FIG. 6. Quantity $d(\eta)=n(>\eta)^{-1/3}$, the mean comoving separation of knots unwinding after conformal time η vs η in the matter and radiation eras. The slope is used to determine the knot production rate in the scaling solution. Two runs were 100^3, the third 60^3 to check for finite-size effects. The slope is used to determine the knot production rate in the scaling solution.

Since the characteristic scale is always the horizon scale, the scaling solution predicts the number of knots unwinding in the interval η to $\eta+d\eta$ per unit comoving volume should scale with η:

$$\frac{dn}{d\eta}=\frac{\nu}{\eta^4}\ , \tag{10}$$

where ν is a dimensionless constant related to the probability of winding around the three-sphere in a correlation volume.[3]

In the simulations we locate the collapsing knots at every time step by identifying all disjoint grid points where $|\phi|<0.5\phi_0$. The norm of the field deviates significantly from ϕ_0 only in regions where the texture is unwinding. Not counting knots that were identified in the previous time step, we compute $dN/d\eta$, the number of knots unwinding in each time step. Each texture knot in the simulation spends approximately three time steps unwinding. We only begin counting knots after three units of conformal time to exclude initial transient behavior.

We ran two 100^3 simulations with the same initial conditions for both matter and radiation-dominated epochs. In a 100^3 simulation beginning at $\eta=1$, around 10^4 knots unwind after $\eta=3$, when we begin counting. In Fig. 6 we plot $d(\eta)$, the cube root of the (comoving) volume of the simulation V divided by the number of knots collapsed after conformal time η:

$$d(\eta)=V^{1/3}\left[\int_\eta^\infty \frac{dN}{d\eta}d\eta\right]^{-1/3}=n(>\eta)^{-1/3}\ . \tag{11}$$

We chose to plot this quantity because the scaling solution implies that $d(\eta)=(3/\nu)^{1/3}(\eta+\eta_0)$, where η_0 is a delay due to the initial "roll-down" stage, lasting a time of order W_0. $d(\eta)$ actually measures the mean comoving separation of knot centers for all knots produced after η. Both simulations are remarkably similar in these units and yield a slope corresponding to $\nu\approx 0.04$. The smallness of ν, implying the rarity of textures, is probably due to geometric factors.[3] Both runs are consistent with the predicted straight-line behavior; the offset $\eta_0\simeq 2$ is close to W_0, as expected. To further test this, we compared two 60^3 runs with identical initial conditions, but with a W_0 of 2 and 4, respectively. As expected, the run with $W_0=4$ had approximately twice as long a "delay" before settling into the scaling solution.

We also performed a two-dimensional simulation of textures for a three-component field with vacuum V_0 a two-sphere. In this case we had much better statistics and could reliably compute the correlation between the location of collapsing knots, well into the simulation, at $\eta=10.0$. The results are shown in Fig. 7. Textures are clearly anticorrelated on scales smaller than the horizon scale. This is quite plausible: The texture field is correlated on the horizon scale, and one is very unlikely to find two knots closer than this.

The rarity of texture knots implies that there should be very few microwave-background hot and cold spots. In Ref. 5 we showed that photons that pass through a collapsing texture knot are redshifted, while those that travel through a region in which a knot has just collapsed are blueshifted. The strongly peaked overdensities generated by texture knots will produce significant early star and quasar formation, certainly in a universe dominated by cold dark matter. These objects are likely to re-ionize the universe and shift the last scattering surface forward to $(1+z)_{\rm sc}\approx 50(\Omega_b h/0.05)^{-2/3}$, where Ω_b is the contribution of baryons to the closure density of the Universe. The number of hot and cold spots on the microwave sky, $N_{\rm spot}$, depends on the number density of knots along the line of sight back to the last scattering surface:

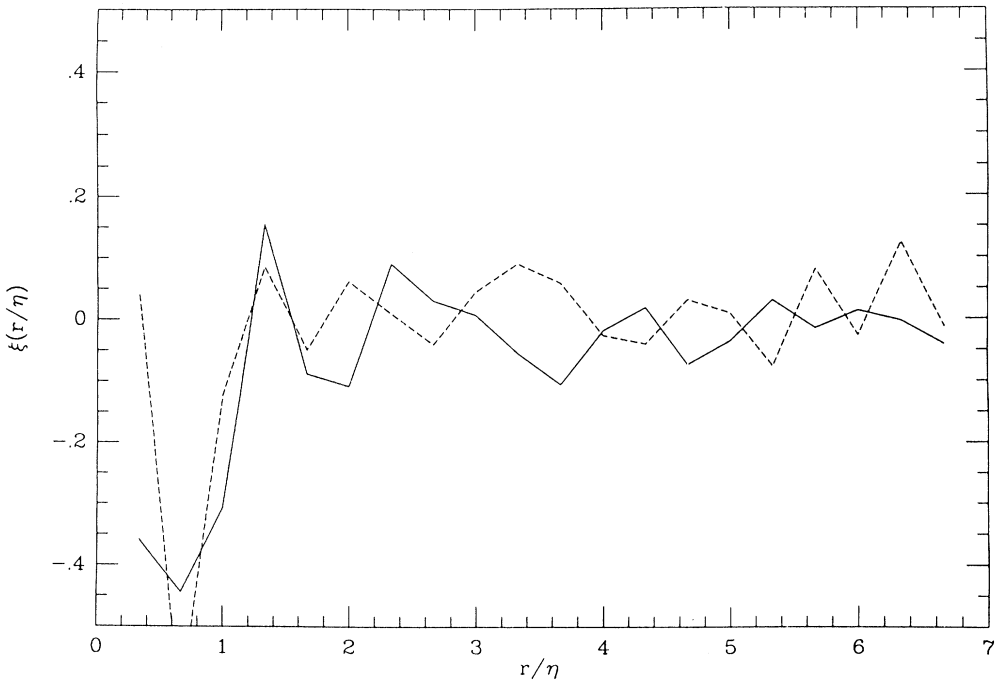

FIG. 7. Two-point spatial correlation function of unwinding knots as calculated for two-dimensional texture. The knots are anticorrelated on scales smaller than the horizon η and uncorrelated on larger scales. r is comoving separation, while η is conformal time.

$$N_{\rm spot}=4\pi\eta_0^2\int_{\eta_{\rm sc}}^{\eta_0}\frac{dn}{d\eta}\eta\,d\eta$$
$$=2\pi\nu\left[\frac{\eta_0}{\eta_{\rm sc}}\right]^2 \qquad (12)$$
$$=2\pi\nu(1+z)_{\rm sc}\ ,$$

where η_0 is the present conformal time. Most of these knots will have angular size $(1+z)_{\rm sc}^{-1/2}$ rad. These numbers correspond to approximately ten hot and cold spots with angular radius of order 8°. Thus texture models are likely to produce a very small quadrupole distortion.

V. CONCLUSION

Our main conclusion is that evolution of global texture is both conceptually simple and numerically tractable. This makes the calculation of large-scale structure predicted from texture quite feasible. The dominant feature of texture evolution and structure formation is knot collapse: Once there is significant ($\simeq 0.5$) winding number within the horizon, the region collapses inward, shrinks to the inverse Higgs-boson mass scale, and then unwinds. During the collapse, the texture appears to approach the exact self-similar flat-space solution described in Ref. 5.

The number of knots unwinding per unit comoving volume in a conformal time interval $d\eta$ scales with η: $dn/d\eta=\nu\eta^{-4}$. Our numerical simulations find that $\nu=0.04$ during both the radiation- and matter-dominated epochs. The energy density in texture Goldstone bosons obeys a simple scaling, corresponding to the texture field being correlated on the horizon scale.

The rarity of texture knots implies that the microwave sky is likely to contain only ~ 10 hot and cold spots, each of angular radius $\sim 8°$. This implies that texture-seeded galaxy formation would produce a very small anisotropy quadrupole and suggests that even texture-seeded galaxy formation in an $\Omega=\Omega_b=0.1$ universe might be consistent with the observational limits on the microwave background. The amplitude of the hot and cold spots depends on the normalization of ϕ_0, which will be treated in Ref. 9.

Asymmetries in the Goldstone-boson energy distribution seem to be damped as knots collapse, so that collapsing knots appear to approach the spherical scaling solution. This suggests that the solution is an attractor. We hope to address this issue in a subsequent paper.[10]

The collapsing knots produce nearly spherical overdensities with $\delta\rho/\rho\propto r^{-1}$. The overdensities collapse and could seed the formation of galaxies and clusters. In a forthcoming paper[9] we will describe the evolution of large-scale structure using the texture simulations to generate the initial conditions in a cold-dark-matter-dominated universe.

ACKNOWLEDGMENTS

The work of D.N.S. was supported by Grant No. AST88-58145 (PYI) and the Alfred P. Sloan Foundation. The work of N.T. was supported by NSF Contract No. PHY80-19754 and the Alfred P. Sloan Foundation.

[1]P. J. E. Peebles and J. Silk, Nature (London) **346**, 233 (1990).
[2]J. R. Bond, Canadian Institute for Theoretical Astrophysics report, 1990 (unpublished).
[3]N. Turok, Phys. Rev. Lett. **63**, 2625 (1989).
[4]M. Barriol and A. Vilenkin, Phys. Rev. Lett. **63**, 341 (1989).
[5]N. Turok and D. Spergel, Phys. Rev. Lett. **64**, 2736 (1990).
[6]W. H. Press, B. S. Ryden, and D. N. Spergel, Astrophys. J. **347**, 590 (1989); **357**, 293 (1990).
[7]T. H. R. Skyrme, Proc. R. Soc. London **A260**, 127 (1961).
[8]R. Durrer, Phys. Rev. D **42**, 2533 (1990).
[9]C. Park, D. Spergel, and N. Turok (unpublished).
[10]A. Gooding, D. Spergel, and N. Turok (unpublished).
[11]See, e.g., R. Rajaraman, *Solitons and Instantons* (North-Holland, Amsterdam, 1982).
[12]S. Veeraraghavan and A. Stebbins, Canadian Institute for Theoretical Astrophysics report, 1990 (unpublished).
[13]L. Kawano, Fermilab report, 1990 (unpublished).